

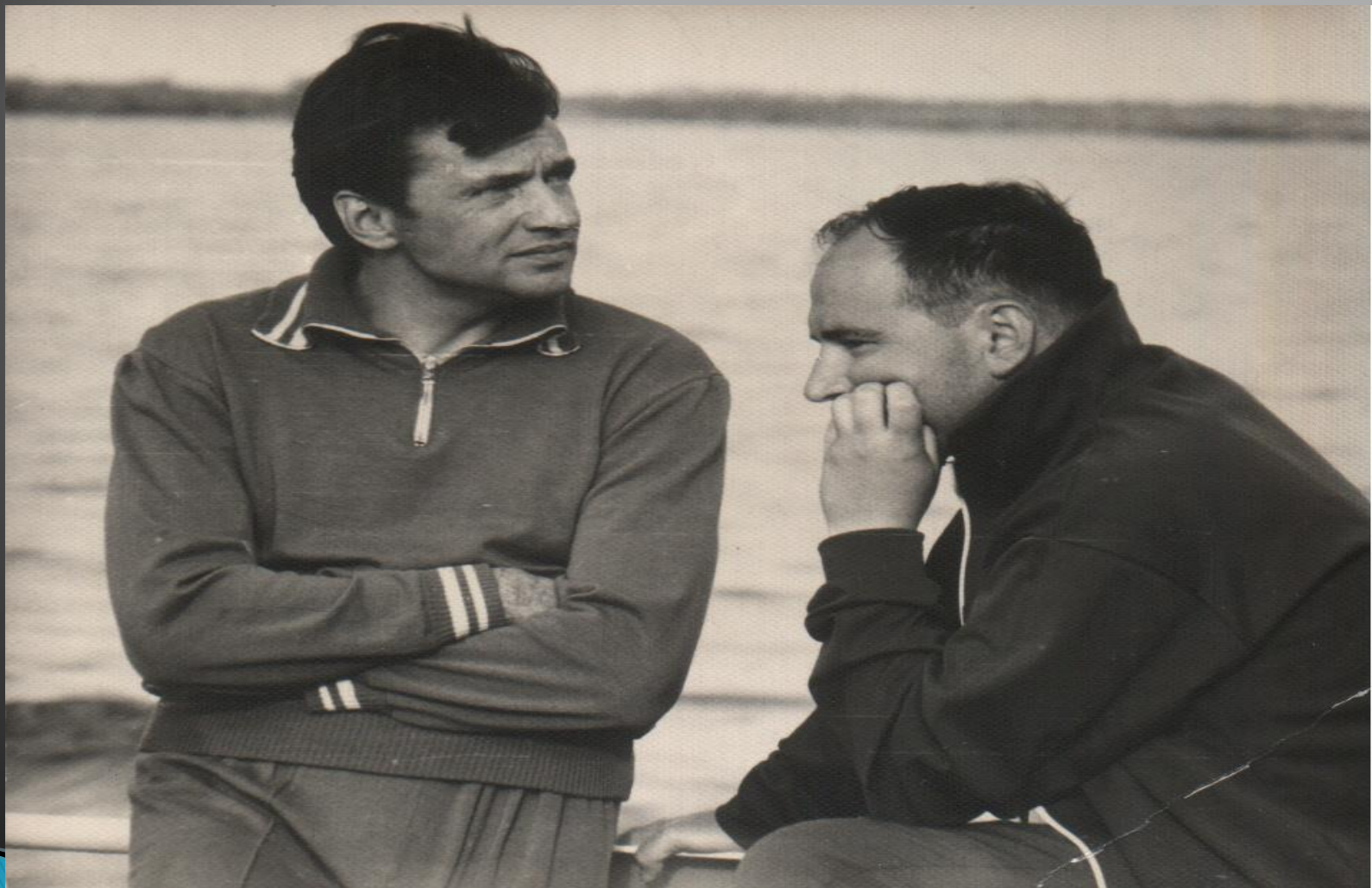
Ионосферный отклик на природные и антропогенные воздействия

О. А. Похотов
Институт физики Земли РАН

Short history

- ▶ The idea of IAR was suggested by Polyakov [1976]
- ▶ First experimental evidence: Polyakov and Rapoport [1981], Belyaev et al. [1987]
- ▶ Recent experimental studies: Belyaev et al. [1999], Demekhov et al. [2000], Bosinger et al. [2002]
- ▶ Theoretical model of the IAR was first developed by Trakhtengertz and Feldstein [1987,1991] and Lysak [1991]
- ▶ Recent progress in the theory: Pokhotelov et al. [2000, 2001, 2003, 2004], Lysak and Song [2002, 2003], Pilipenko et al. [2002], Streltsov et al. [2002], Surkov et al. [2004]

Trakhtengertz V and & Feldstein Y



Basic contributions

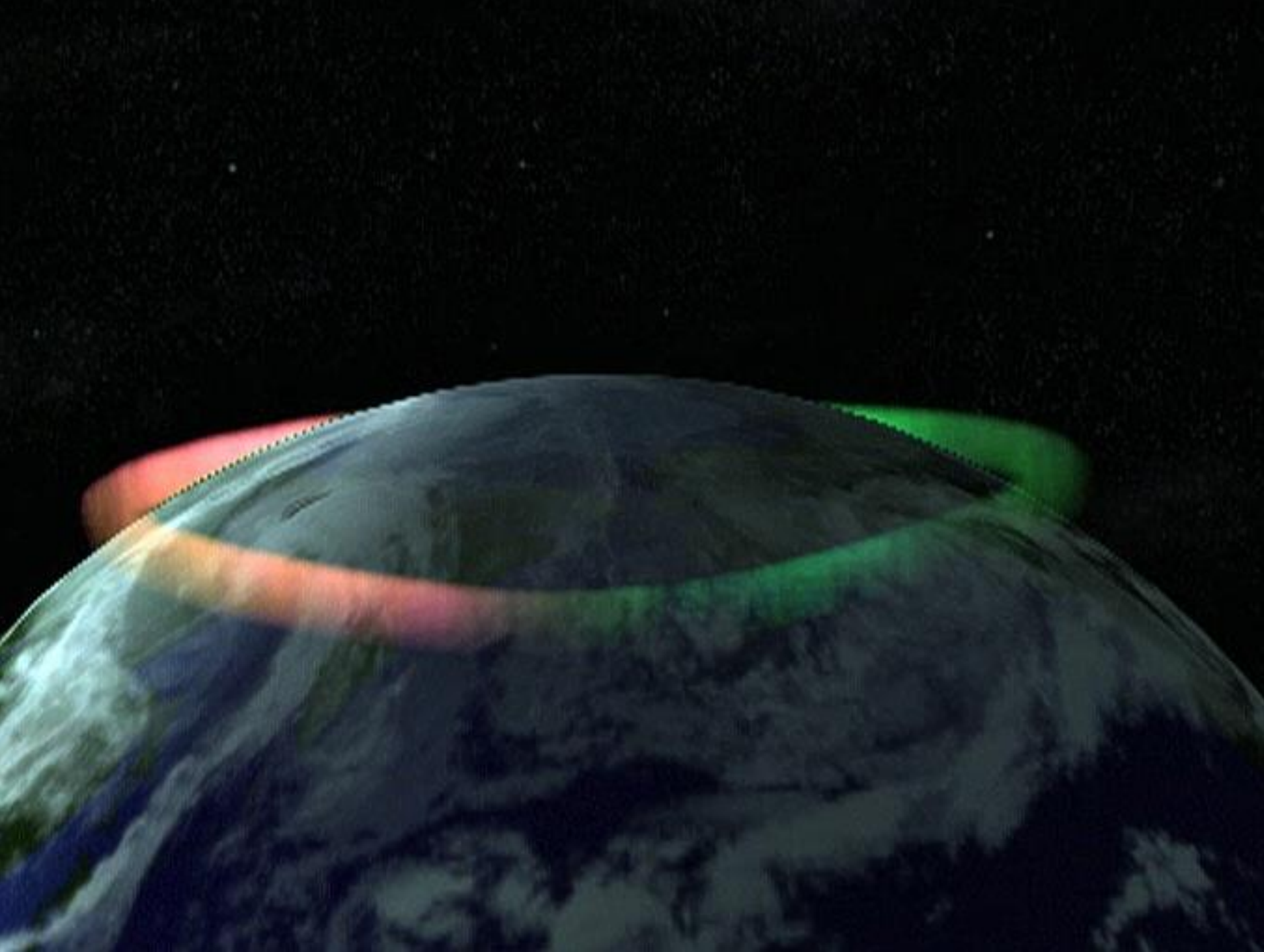
Feldstein Y. I. – SCI – 1970

Feldstein & Starkov, Dynamics of auroral belt and polar geomagnetic disturbances, (PSS, 1967). SCI – 321.

Trakhtengertz V. Y. – SCI – 1208

Trakhtengertz V. Y. & Feldstein A. Y., Quiet auroral arcs – ionospheric effect of magnetospheric convection, PSS, 1984.

Turbulent Alfvén boundary layer..., 1991.

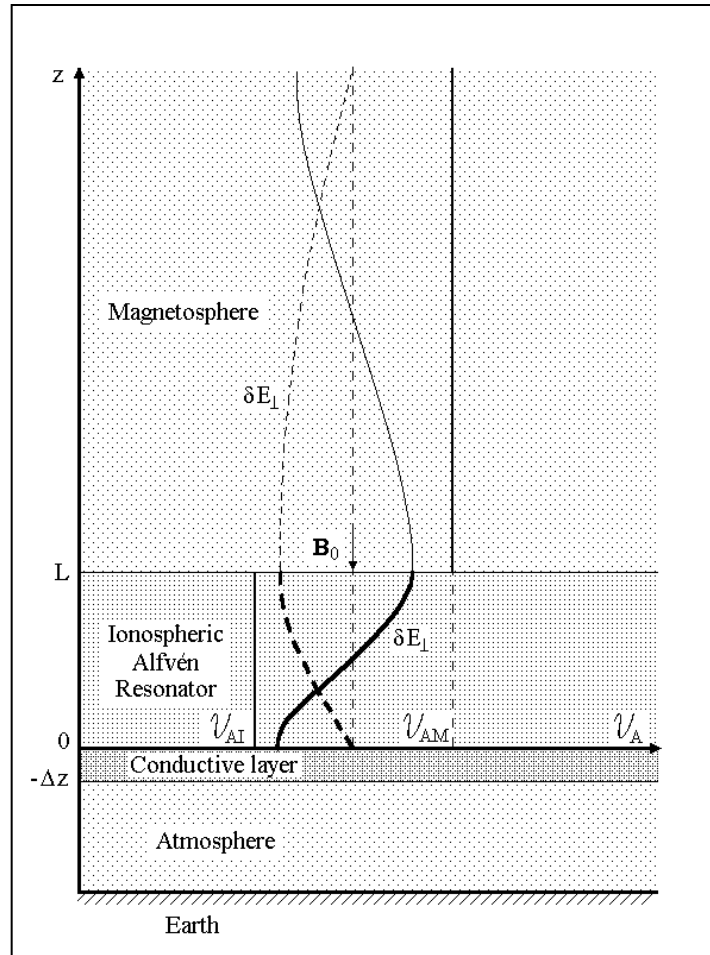


Авроральное колечко Ольги
Хорошевой
(1961, НИИЯФ МГУ)





Schematic view



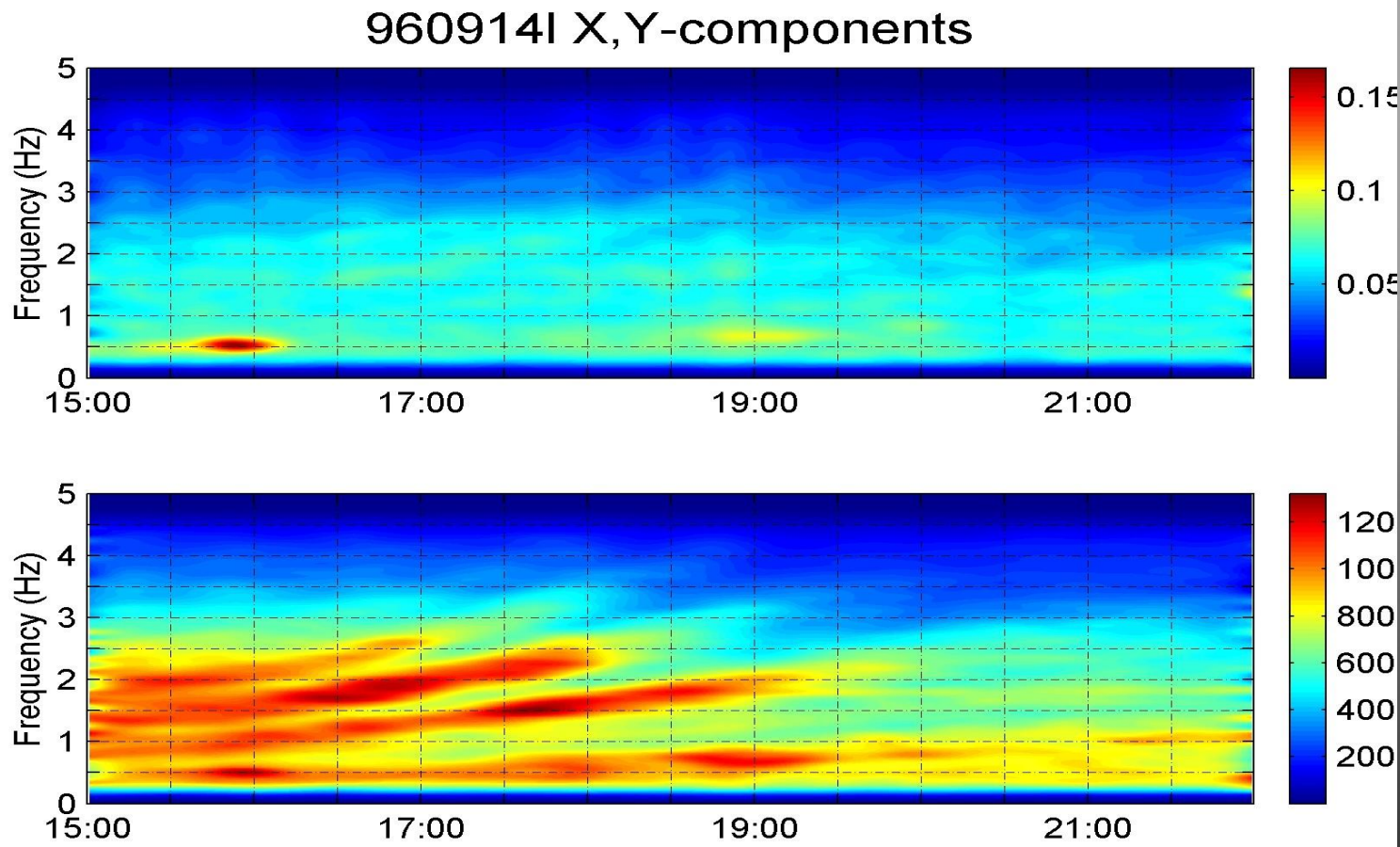
Ground and satellite observations

- ▶ Nizniy–Novgorod
(Middle Russia)
- ▶ Borok (Middle
Russia)
- ▶ Mondy (Siberia,
Russia)
- ▶ Karimshino
(Kamchatka, Russia)
- ▶ Sodankyla (Finland)
- ▶ Crete (Greece)
- ▶ Table Mountain
obs., USA
- ▶ FREJA satellite
- ▶ FAST satellite
- ▶ CLUSTER satellites
- ▶ DEMETER

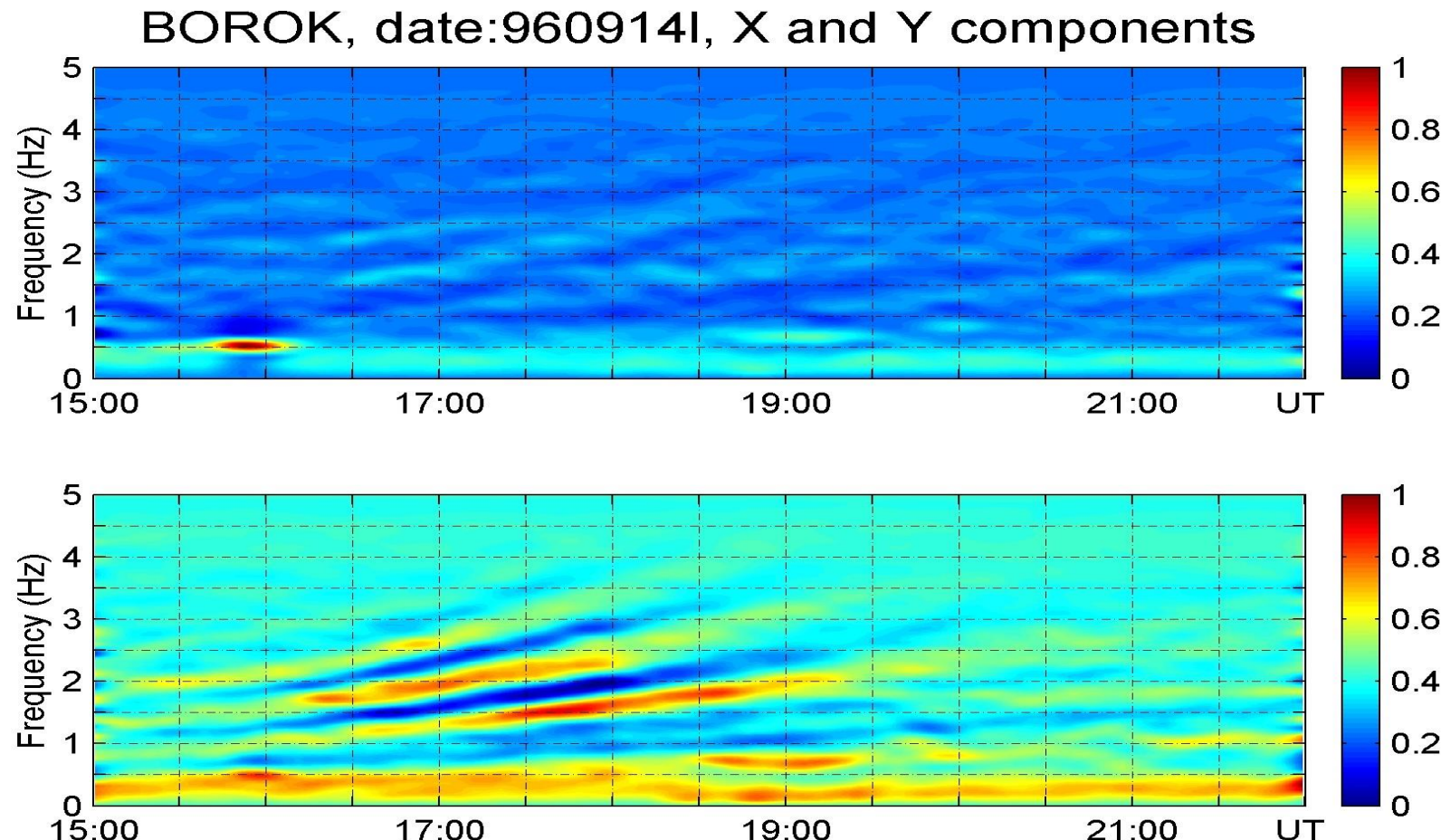
Sources of free energy for the IAR excitation

- ▶ High-latitudes –
Magnetospheric convection
(feedback instability)
- ▶ Middle-latitudes –
Thunderstorm activity
- ▶ Neutral winds, Subauroral
Polarization Streams (SAPS)

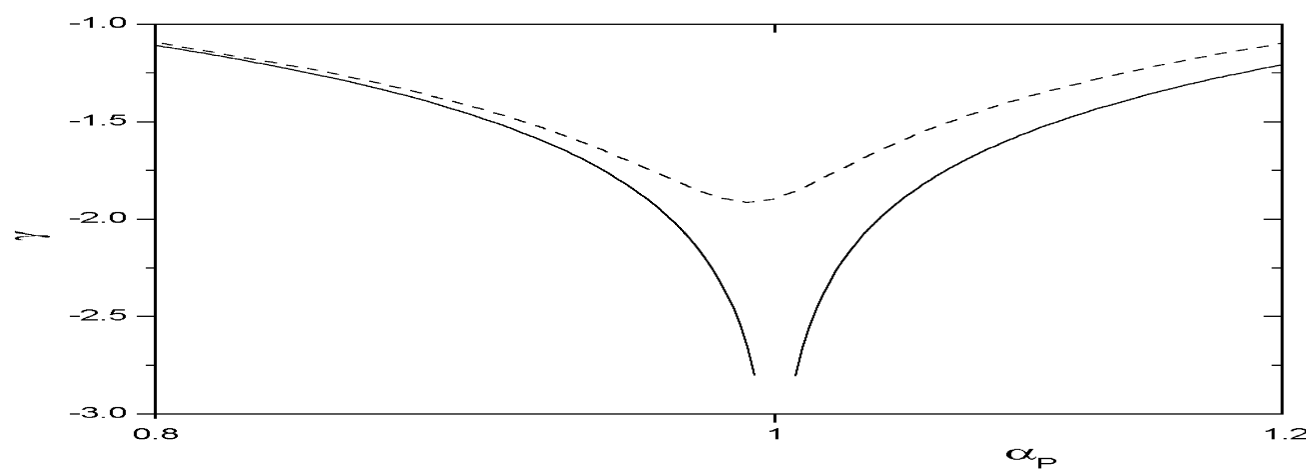
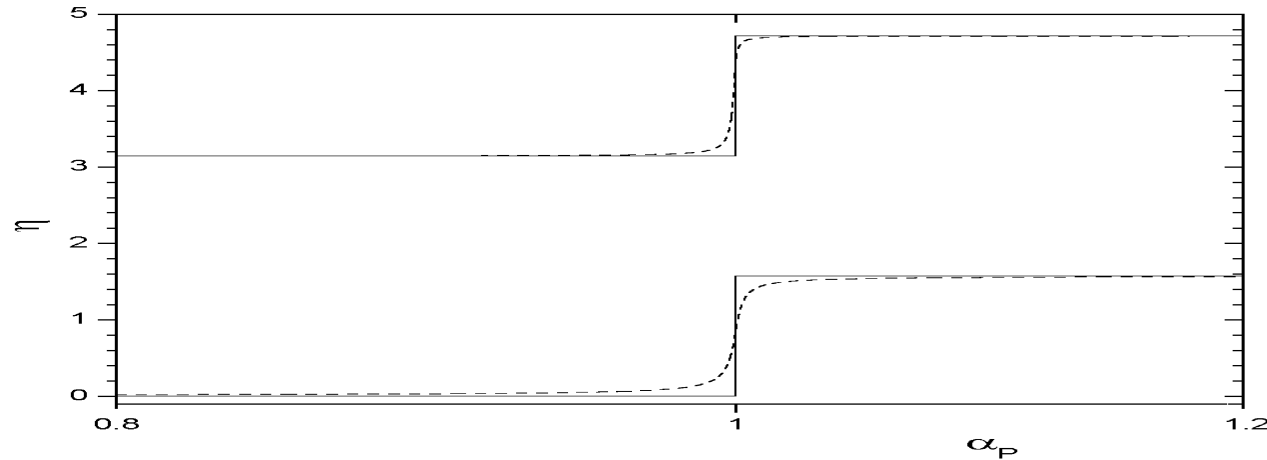
Ground observations of SRS



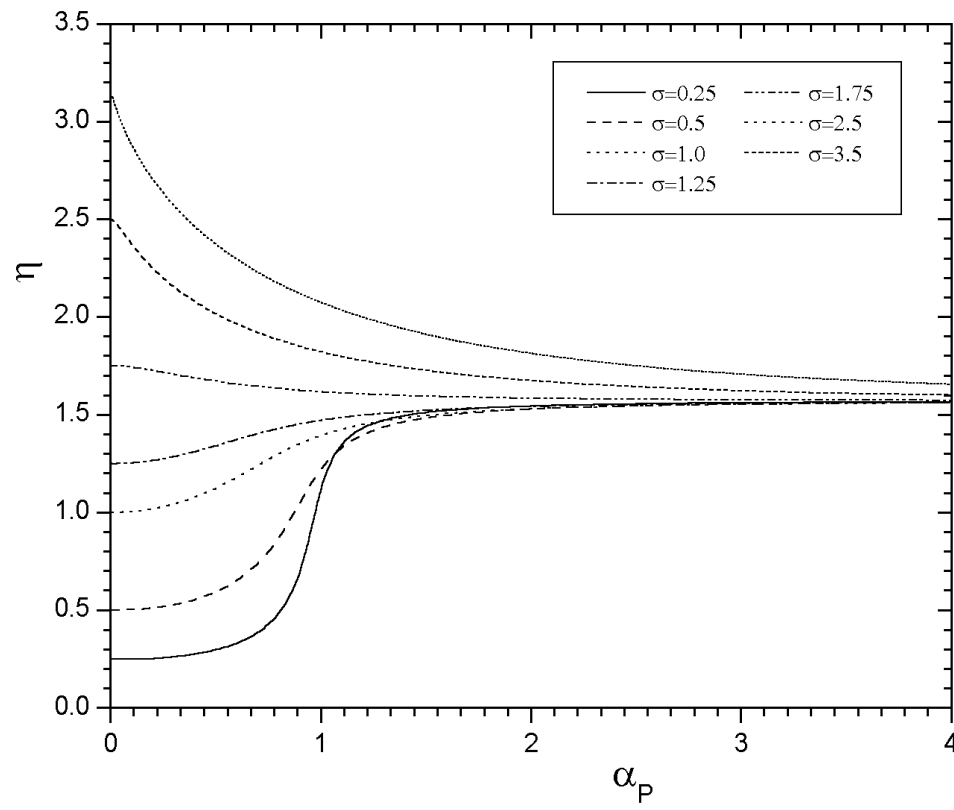
Ground observations of SRS



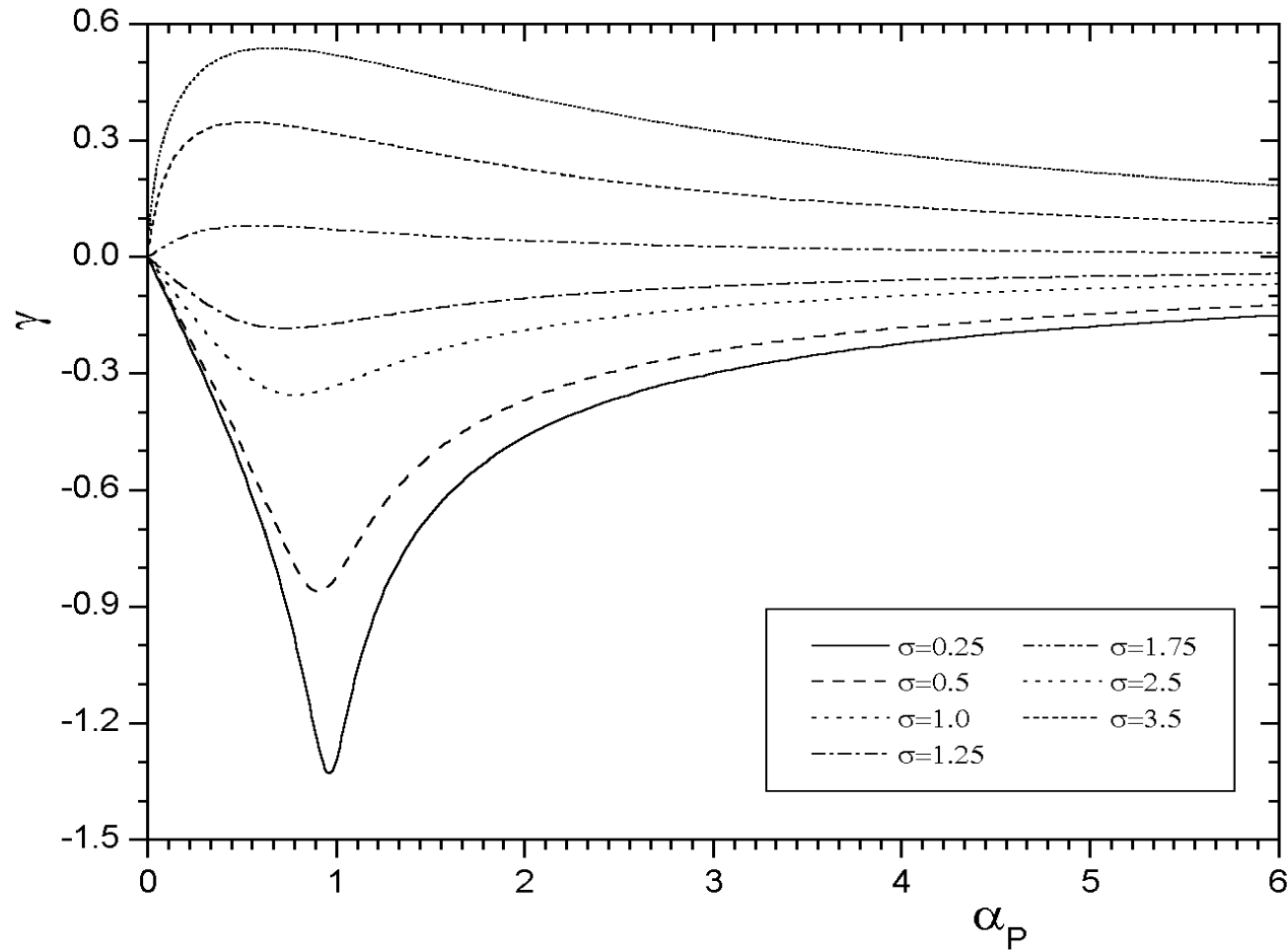
IAR Eigenmodes and damping rates



Eigen-frequencies



Variation of the damping/growth rate in the presence of magnetospheric convection



Basic NL equations

Potentials

$$E_z = \mathbf{E} \cdot \hat{\mathbf{z}} = -\partial_z \varphi - \partial_t A \quad \mathbf{E}_\perp = -\nabla_\perp \varphi,$$

$$\mathbf{B}_\perp = \nabla A \times \hat{\mathbf{z}} \quad E_{II} = E_z + \frac{\mathbf{B}_\perp \cdot \mathbf{E}_\perp}{B_0} = D_t A - \partial_t \varphi$$

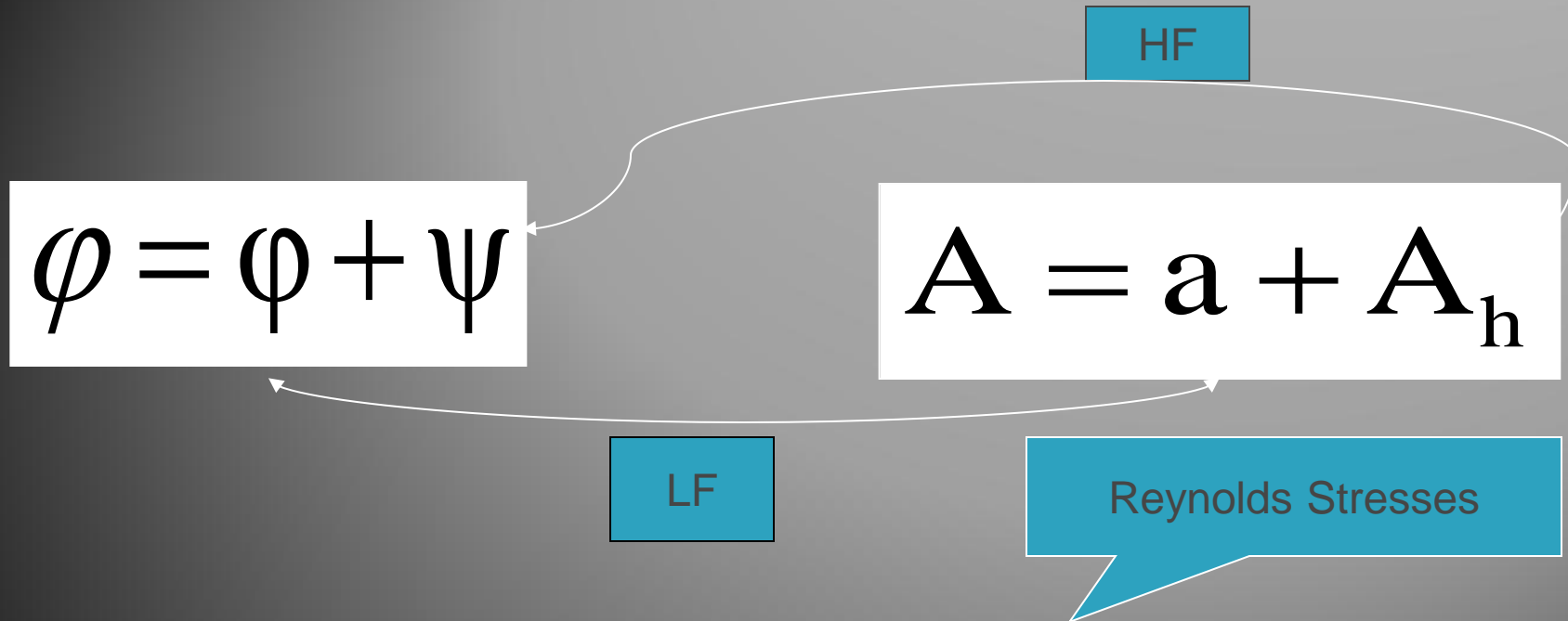
$$D_t = \partial_t + B_0^{-1} \{ \varphi, \dots \} \quad \{ A, B \} = (\partial_x A) \partial_y B - (\partial_y A) \partial_x B$$

Nonlinear equations

■ $D_t \nabla_\perp^2 \varphi + v_A^2 D_z \nabla_\perp^2 A = 0,$ $D_z \equiv \partial_z + B_0^{-1} \mathbf{B}_\perp \cdot \nabla$

■ $D_t (1 - \lambda_e^2 \nabla_\perp^2) A + \partial_z \varphi = 0.$

Multiscale expansion



$$\partial_t \nabla_{\perp}^2 \varphi = -B_0^{-1} (\langle \{\psi, \nabla_{\perp}^2 \psi\} \rangle - v_A^2 \langle \{A, \nabla_{\perp}^2 A\} \rangle)$$

$$\partial_t (1 - \lambda_e^2 \nabla_{\perp}^2) a = -B_0^{-1} \langle \{\psi, (1 - \lambda_e^2 \nabla_{\perp}^2) A\} \rangle$$

Quasi-monochromatic approach

$$(\phi, a) = (\phi_{\mathbf{q}}, A_{\mathbf{q}}) \exp[i(\mathbf{q} \cdot \mathbf{r} - \Omega t)] + c.c.$$

$$\psi = \psi_0 + \psi_+ + \psi_-$$

$$A = A_0 + A_+ + A_-$$

$$(\psi_0, A_0) = (\psi_{\mathbf{k}}, A_{\mathbf{k}}) \exp[i(\mathbf{k} \cdot \mathbf{r} - \omega_{\mathbf{k}} t)] + c.c.$$

$$(\psi_{\pm}, A_{\pm}) = (\psi_{\mathbf{k}\pm}, A_{\mathbf{k}\pm}) \exp[i(\mathbf{k}_{\pm} \cdot \mathbf{r} - \omega_{\mathbf{k}\pm} t)] + c.c$$

$$\omega_{\mathbf{k}\pm} = \omega_{\mathbf{k}} \pm \Omega$$

$$\mathbf{k}_{\pm} = \mathbf{k} \pm \mathbf{q}$$

Convective cells generation

Dispersion relation

$$\Omega_{\pm} = \mathbf{q} \cdot \mathbf{v}_g \pm i[b(\mathbf{q} \times \mathbf{k})_z^2 |\psi_0|^2 B_0^{-2} - \delta\omega^2]^{1/2}$$

$$b = k^2 \lambda_e^2 (1 + k^2 \lambda_e^2)^{-1}$$

$$\delta\omega \approx b\omega_k q^2 / 2k^2$$

Optimal dimensions

$$\left(\frac{\mathbf{q}}{k}\right)_{\max}^2 = \frac{2(1 + k^2 \lambda_e^2)^3 |B_k|^2}{k_z^2 \lambda_e^2 B_0^2}$$

Maximum growth rate

$$\frac{\gamma_{\max}}{\omega_k} = (1 + k^2 \lambda_e^2)^3 \frac{k^2 |B_k|^2}{k_z^2 B_0^2}$$

Competing mechanisms

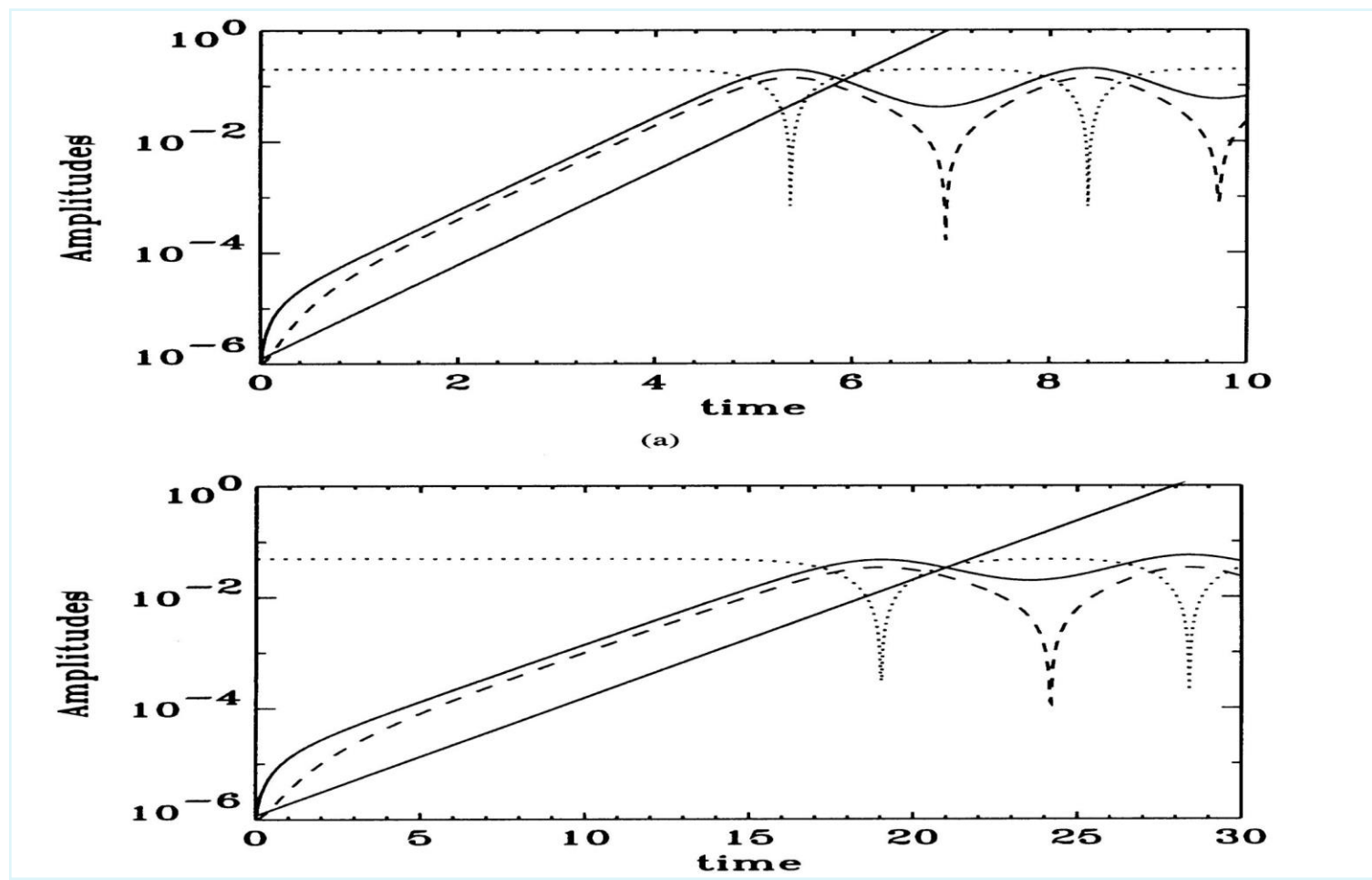
$$\text{IAW} = \text{IAW} + \text{IAW}$$

$$\gamma_{AA} = 0.15 v_A \lambda_e k_\perp^2 \left| \frac{\mathbf{B}_k}{B_0} \right|^{-1}$$

$$\frac{\gamma_{AA}}{\gamma_{cell}} = 0.15 \frac{k_z \lambda_e}{(1 + k_\perp^2 \lambda_e^2)^{3/2}} \left| \frac{\mathbf{B}_k}{B_0} \right|^{-1}$$

$$\frac{k_z}{k(1 + k^2 \lambda_e^2)} > \left| \frac{\mathbf{B}_k}{B_0} \right| > 0.15 \frac{k_z \lambda_e}{(1 + k^2 \lambda_e^2)^{3/2}}$$

Numerical Simulation



Suppression of the parametric instability in the auroral cavity

$$d_t(1 - \lambda_e^2 \nabla_{\perp}^2)A + \partial_z \varphi = 0$$

$$\frac{v_A^2}{c^2} \partial_t \nabla_{\perp}^2 \varphi + d_t \nabla_{\perp}^2 \varphi + v_A^2 d_z \nabla_{\perp}^2 A = 0$$

Relativity of the
Alfven velocity

$$\gamma = [2q^2 |v_E|^2 (b - 2 \frac{v_A^2}{c^2}) - \delta\omega^2]^{1/2}$$

Other predator-prey models

- ▶ Hasegawa–Mima model for drift turbulence
- ▶ Generation of zonal flows and streamers
- ▶ Bohm–like plasma diffusion
- ▶ Suppression of drift turbulence
- ▶ Charney model for Rossby waves
- ▶ Generation of zonal and meridional flows

Experimental evidence

Magnetosonic ULF waves generated by modulated ionospheric heating using recently completed HAARP heater were measured on board the DEMETER spacecraft. Modulated F-region ionospheric heating thus provides us with the first artificial Pc 1 source that can propagate laterally in the ionospheric waveguide.

HAARP (High Frequency Active Auroral Research Program)

The project started in spring 1997, Gakona Alaska

Similar projects

Russia (Vasilyevsk) – SURA

Ukraine – Kharkov region

Tajikistan – Dushanbe

Peru – Jicamarca Radio observatory

Emission power

HAARP (Gakona, Alaska) – 3600 kW

EISCAT (Tromsø, Norway) – 1200 kW

SPEAR (Longyear, Norway) – 288 kW

HAARP



Riometer



Basic equations (ionosphere)

Ampere's law

$$(\nabla \times \delta \mathbf{B})_{\perp} = \mu_0 (\mathbf{J}_{\perp} + \mathbf{J}_H) + \frac{K(z)}{c^2} \frac{\partial \mathbf{E}_{\perp}}{\partial t}$$

Here

$$\mathbf{J}_{\perp} = \sigma_P \mathbf{E}_{\perp} + \sigma_H \mathbf{z} \times \mathbf{E}_{\perp} \text{ and } \mathbf{J}_H = (\mathbf{B} \times \nabla \delta p) / B^2$$

Faraday's law

$$\nabla \times \mathbf{E} = - \frac{\partial \delta \mathbf{B}}{\partial t}$$

Parallel electron motion

$$\mathbf{E}_P = \mu_0 \lambda^2 \left(\frac{\partial}{\partial t} + v_e \right) \mathbf{J}_P$$

$$K(z) = 1 + \sum_j \frac{\omega_{pj}^2}{v_j^2 + \omega_{cj}^2}$$

$$\sigma_P(z) = \sum_j \frac{n_{0j} q_j^2}{m_j} \frac{v_j}{v_j^2 + \omega_{cj}^2}$$

$$\sigma_H(z) = - \sum_j \frac{n_{0j} q_j^2}{m_j} \frac{\omega_{cj}}{v_j^2 + \omega_{cj}^2}$$

Dimensionless form

$$\begin{aligned}\left[\frac{\partial}{\partial \tau} + \alpha_p(\zeta) \right] q &= -\frac{1}{K(\zeta)} \frac{\partial j}{\partial \zeta} m \alpha_h(\zeta) m \\ \left[\frac{\partial}{\partial \tau} + \alpha_p(\zeta) \right] m &= -\frac{1}{K(\zeta)} \nabla^2 b \pm \alpha_h(\zeta) q \\ -\frac{\beta}{2K(\zeta)} \nabla_{\perp}^2 \frac{\delta p}{p_0} &\end{aligned}$$

$$\begin{aligned}\frac{\partial b}{\partial \tau} &= -m \\ \frac{\partial}{\partial \tau} \left(1 - \frac{m_e}{m_i} \nabla_{\perp}^2 \right) j &= -\frac{\partial q}{\partial \zeta} + \frac{v_e}{\omega_{ce}} \nabla_{\perp}^2 j\end{aligned}$$

$$\begin{aligned}q &= \frac{c}{\omega_{pi}^I} \frac{\nabla_{\perp} g \mathbf{E}_{\perp}}{B v_A^I} & m &= \frac{c}{\omega_{pi}^I} \frac{(\nabla_{\perp} \times \mathbf{E}_{\perp})_z}{B v_A^I} \\ j &= \frac{J_p}{e n_0^I v_A^I} & b &= \frac{\delta B_z}{B}\end{aligned}$$

Atmosphere

$$b(\zeta) = b(H) \frac{k\delta \cosh k\zeta + (1+i) \sinh k\zeta}{k\delta \cosh kH + (1+i) \sinh kH}$$

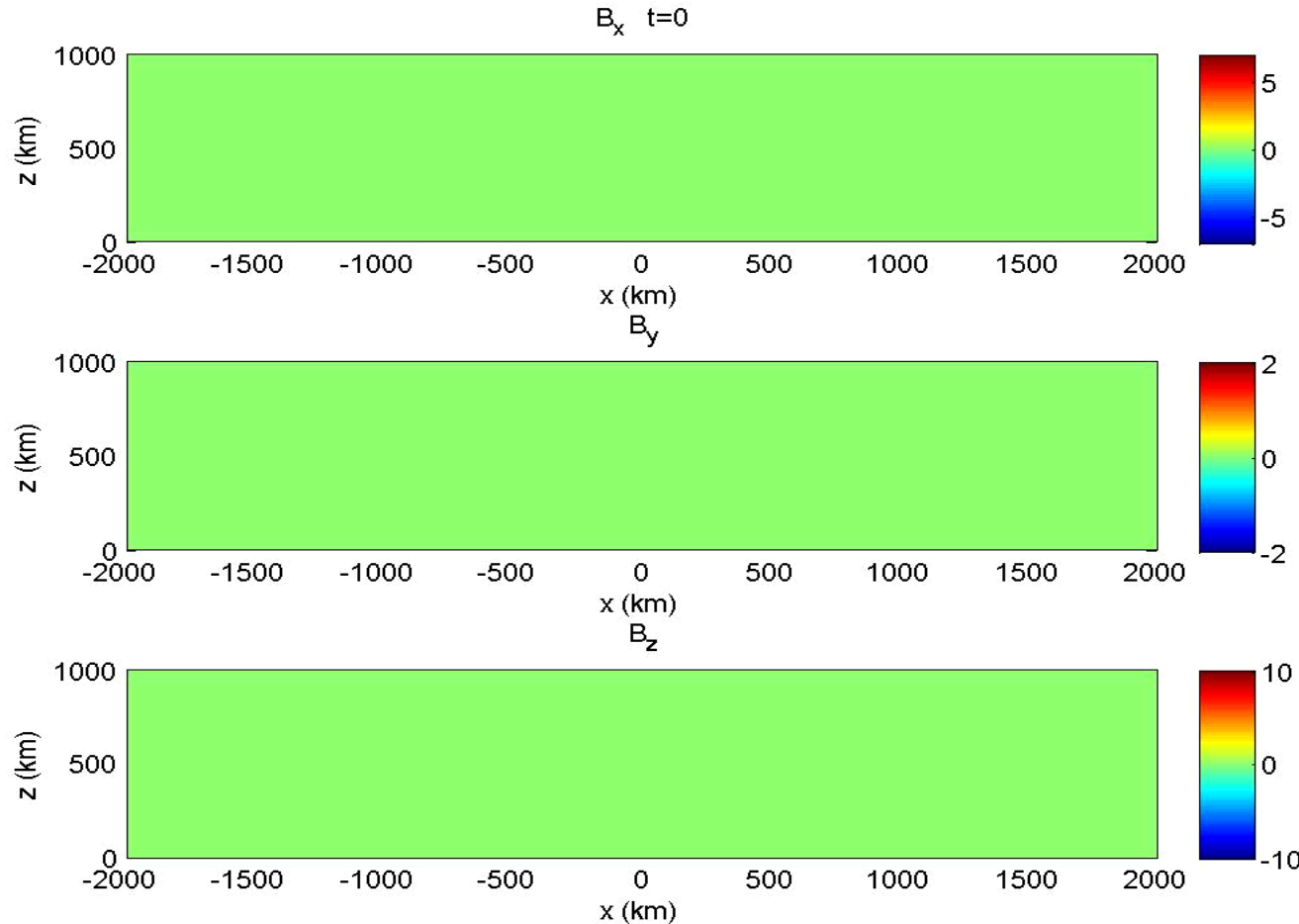
where $\delta = (2 / \omega \mu_0 \sigma_g)^{1/2}$ is the skin depth
of the solid Earth

In the atmosphere $\partial / \partial \tau = 0$

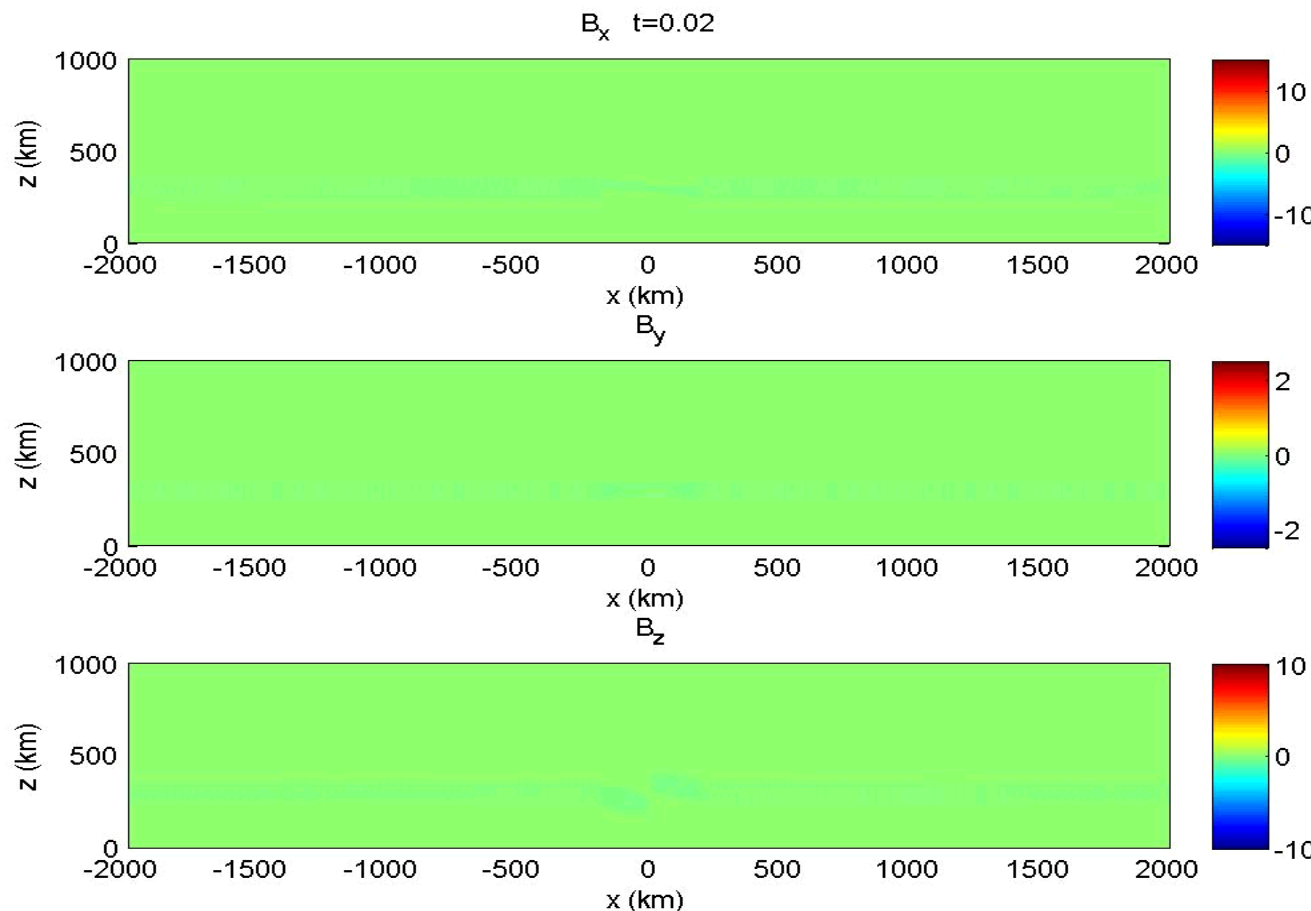
$q = -(\nu_e / \omega_{ce}) \partial j / \partial \tau$ and

$$\frac{\partial}{\partial \zeta} \left(\frac{\nu_e}{\omega_{ce}} \frac{\partial j}{\partial \tau} \right) + \frac{\nu_e}{\omega_{ce}} \nabla_{\perp}^2 j = 0$$

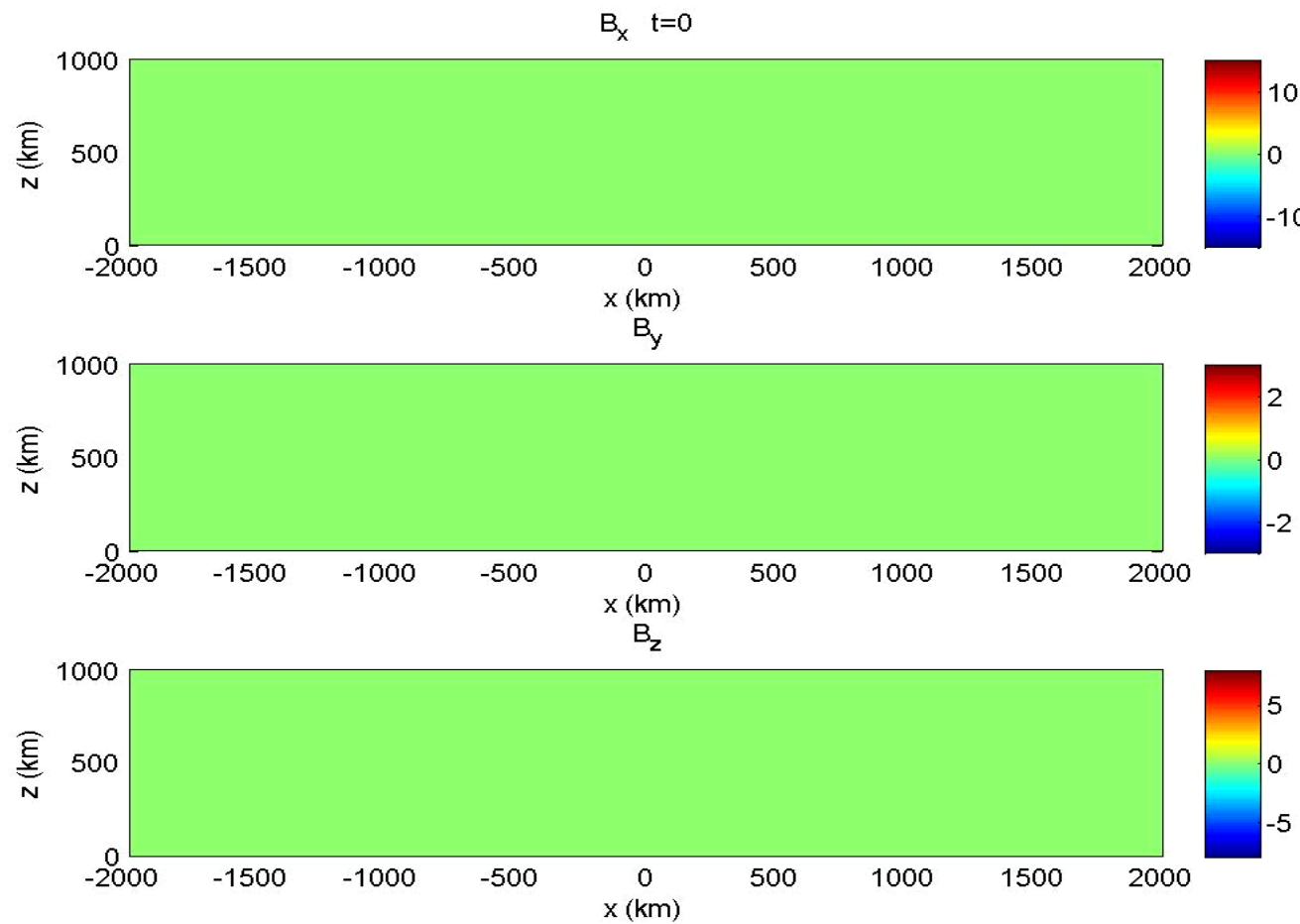
Vertical magnetic field



Oblique MF



Dipole MF



Conclusions

- Alfvén waves excited in the IAR practically never appear as small amplitude linear disturbances
- Parametric instability provides a substantial damping of the IAR eigenmodes and an essential mechanism of energy transfer from small-scale AWs to large and mesoscale convective motions
- The convective cells can interact with the background medium and develop 2D NL motions in the form of Kelvin-Stuart vortex streets
- Such a scenario constitutes a dynamical paradigm for intermittency in the ionospheric turbulence containing nonlinearly coupled AWs and convective motions

Деметер

Запущен 29 июня 2004 г. С космодрома
Байконур. Полярная орбита. Высота 710
км.

Demeter (Detection of Electro-MagneticEmissions Transmitted from Earthquake Regions)

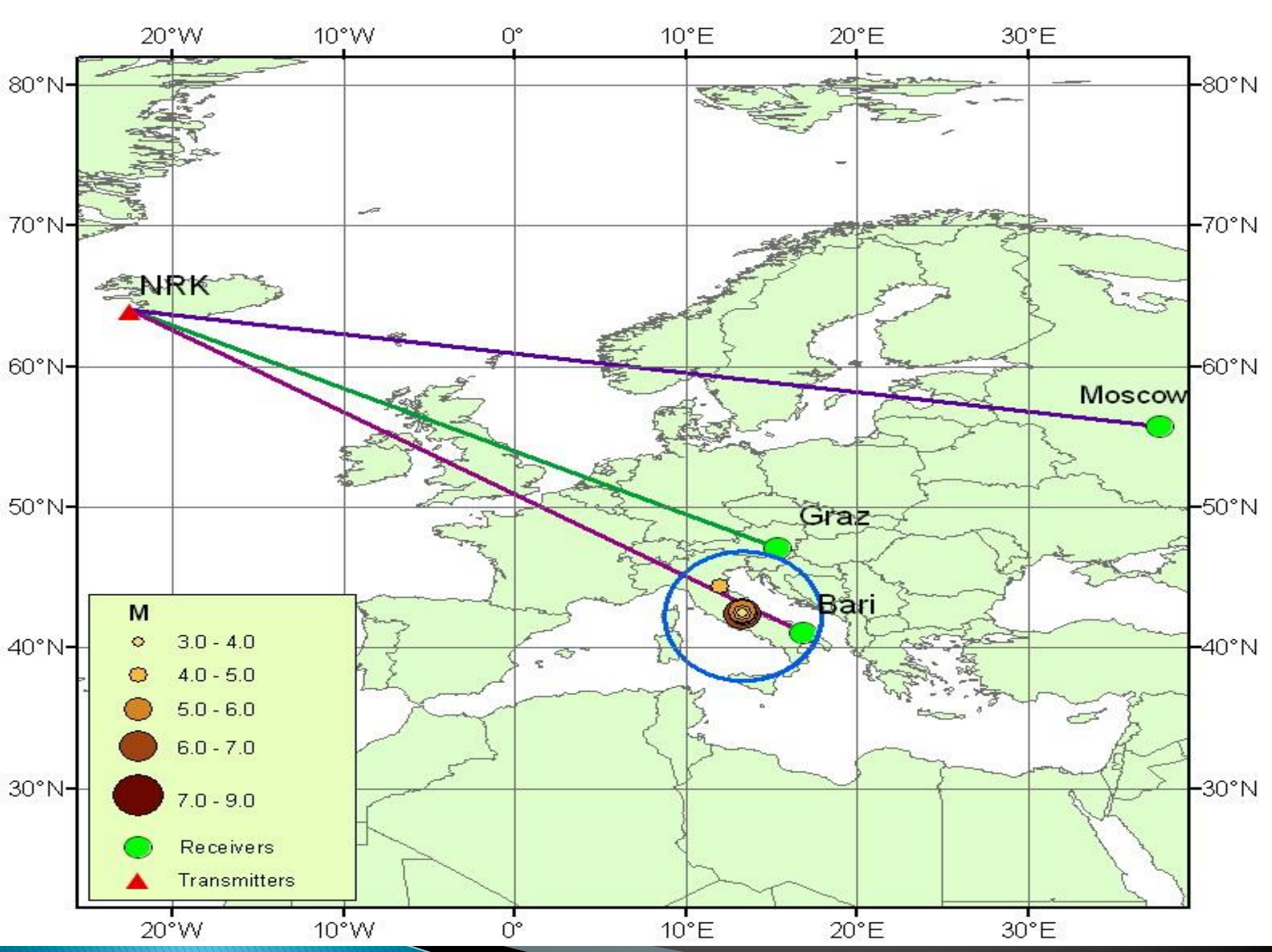


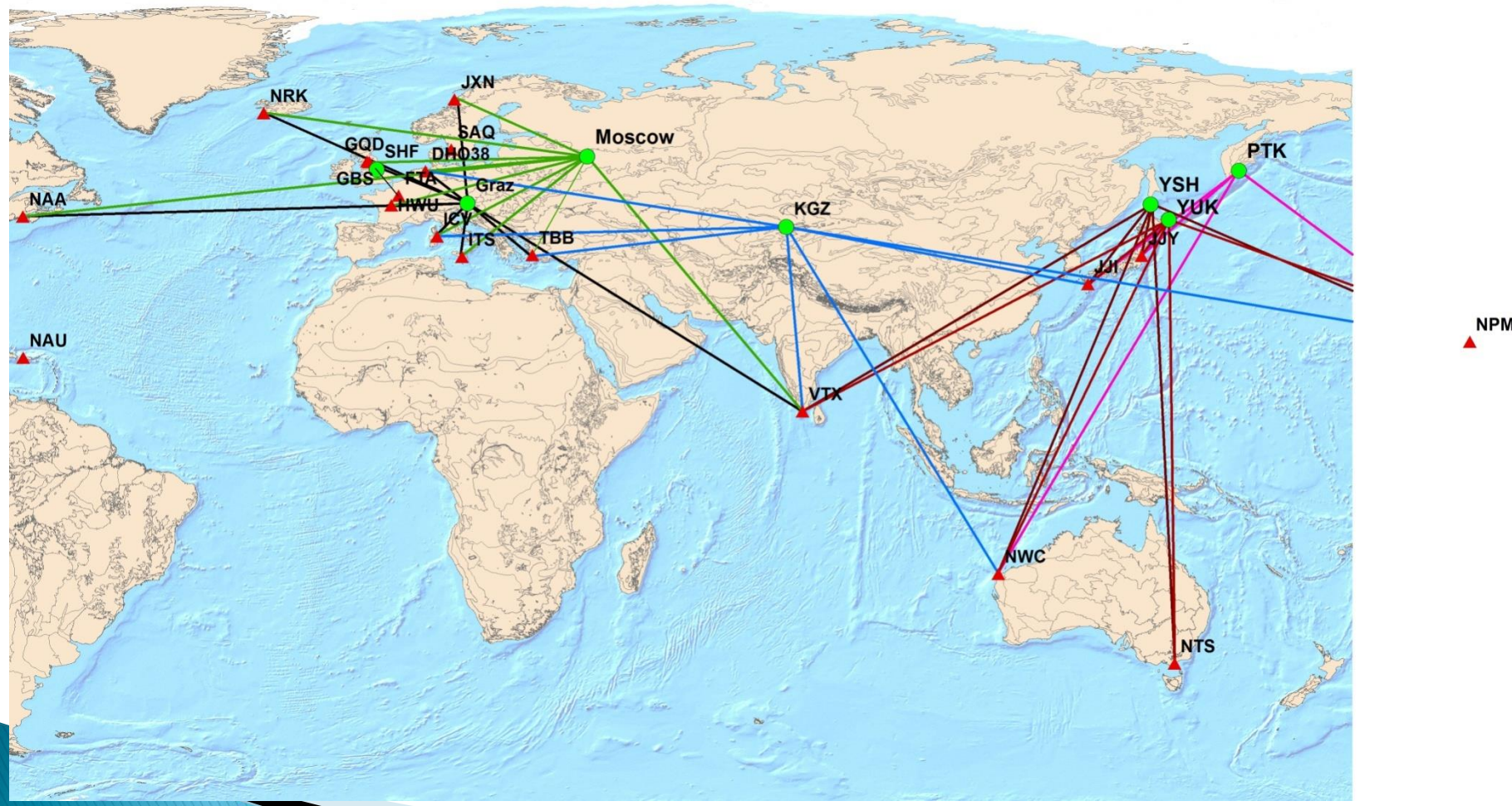
ОНЧ сигнал распространяется между Землей и ионосферой как в сферическом волноводе, нижней стенкой которого является поверхность Земли, а верхней – самая нижняя часть ионосферы – слой D. Эффективная высота отражения сигнала обычно принимается днем 70, а ночью - 90 км. Характер распространения ОНЧ сигнала определяется главным образом величиной и градиентом электронной плотности около границы атмосфера-ионосфера.

Впервые метод мониторинга ОНЧ сигналов системы «ОМЕГА» в связи с сейсмической активностью был применен сотрудниками нашего института:

Gokhberg M.B., Gufeld I.L., Rozhnoy A.A. et al. Study of seismic influence on the ionosphere by super long-wave probing of the Earth –ionosphere wave-guide, *Phys. Earth and Planet. Inter.* 1989. V. 57, № 1-2. P. 64-67.

Гуфельд И.Л., Рожной А.А., Тюменцев С.Н. Возмущения радиоволновых полей перед Рудбарским и Рачинским землетрясениями, *Изв. АН Физика Земли.* 1992, N 3, с. 102-106





The detection of natural disaster precursors through micro- and nano satellite observations in the Earth's ionosphere

Joint Russia – UK satellite project Twinsat





***Thank
you!***